Thus our results prove that C_4 photosynthesis exists in a terrestrial plant without the dual-cell Kranz anatomy system. C_4 photosynthesis is accomplished within a single cell by novel cytological features that allow spatial separation of the biochemical events necessary for operation of the C_4 mechanism. Until now, the separation of functions in terrestrial C_4 plants has been associated only with Kranz-type leaf anatomy. *B. aralocaspica* has evolved a unique solution for the requirement of spatial separation of these biochemical functions within a single cell. PPDK is positioned at the distal part of the cell, where it can generate PEP, the substrate for PEP carboxylase. PEP carboxylase fixes atmospheric CO_2 supplied to the cell through the adjoining intercellular air spaces. NAD-ME and Rubisco are compartmentalized to the interior of the cells, where CO_2 can be donated from C_4 acids to the C_3 pathway. The C_4-type $\delta^{13}C$ values and lack of inhibition of photosynthesis by O_2 demonstrate that CO_2 can be concentrated sufficiently around Rubisco through this specialized compartmentation to minimize photorespiration. The physical requirements for C_4 photosynthesis may be met by the existence of a sufficiently high diffusive resistance in the aqueous phase between sites of CO_2 donation to Rubisco in the proximal ends of the cells and sites of fixation of atmospheric CO_2 by PEP carboxylase at the distal ends.

Our results are relevant to the discussion of evolution of C_4 photosynthesis in plants, because the first land plants were C_3 species[2,4]. C_4 species are an important component of global ecosystems and there is interest in their evolution and the consequences to evolution of mammals[2,4,18,19]. Palaeorecords have been used to study how long C_4 plants have existed on Earth by finding well preserved fossils that have Kranz anatomy and C_4-type isotope composition. Now our results indicate that it is possible that plant fossils with a C_4 isotope composition but without Kranz anatomy may be C_4 species (rather than CAM species).

C_4 plants are also of considerable interest because this mechanism of photosynthesis has an advantage over C_3 plants for conversion of solar energy into biomass in hot, dry and/or saline habitats. Maize, sugarcane and sorghum are important C_4 crop plants, but most agricultural crops, including rice and wheat, are C_3 plants. This has led to interest in genetically engineering C_3 crops to perform C_4 photosynthesis in order to increase productivity[20,21]. Although this may require alterations in anatomy as well as biochemistry, our results indicate that it would not require development of two photosynthetic cell types. □

Methods

Plants were grown under controlled growth conditions with day/night temperatures of 25/18 °C, and a 14/10 h photoperiod, with a stepwise increase and decrease in light intensity during the day to a maximum photosynthetic quantum flux density of 1,100 $\mu mol\ m^{-2}\ s^{-1}$. For immunolocalization studies, samples were prepared as described[10]. Antibodies used were anti-spinach Rubisco (LSU) IgG (courtesy of B. McFadden), anti-maize PPDK IgG (courtesy of T. Sugiyama), anti-maize PEPC IgG (Chemicon), anti-maize NADP-ME IgG with relative molecular mass (M_r) 62,000 (courtesy of C. Andreo[22]), and anti-*Amaranthus hypochondriacus* mitochondrial NAD-ME IgG, which was prepared against the α subunit with M_r65,000 (courtesy of J. Berry[23]). For details of techniques used for immunolocalization by light microscopy see ref. 10. The background labelling with preimmune serum was non-specific and low to nonexistent (results not shown but see ref. 10).

Received 14 August; accepted 18 October 2001.

1. Badger, M. R. & Spalding, M H. in *Photosynthesis: Physiology and Metabolism* (eds Leegood, R. C., Sharkey, T. D. & von Caemmerer, S.) 369–397 (Kluwer Academic, Netherlands, 2000).
2. Sage, R. F. Environmental and evolutionary preconditions for the origin and diversification of the C_4 photosynthetic syndrome. *Plant Biol.* **3,** 202–213 (2001).
3. Hatch, M. D. in *Photosynthesis and Photorespiration* (eds Hatch, M. D., Osmond, C. B. & Slatyer, R. O.) 139–152 (Wiley-Interscience, New York, 1971).
4. Sage, R. F. & Monson, R. K. *C_4 Plant Biology* (Academic, San Diego, 1999).
5. Edwards, G. E. & Walker, D. A. *C_3,C_4: Mechanisms, and Cellular and Environmental Regulation, of Photosynthesis* (Blackwell Scientific, Oxford, 1983).
6. Edwards, G. E., Furbank, R. T., Hatch, M. D. & Osmond, C. B. What does it take to be C_4? Lessons from the evolution of C_4 photosynthesis. *Plant Physiol.* **125,** 46–49 (2001).
7. Winter, K. & Smith, J. A. C. *Crassulacean Acid Metabolism* (Springer, New York, 1996).
8. Freitag, H. & Stichler, W. A remarkable new leaf type with unusual photosynthetic tissue in a central asiatic genus of Chenopodiaceae. *Plant Biol.* **2,** 154–160 (2000).
9. Carolin, R. C., Jacobs, S. W. L. & Vesk, M. The structure of the cells of the mesophyll and parenchymatous bundle sheath of the Gramineae. *Bot. J. Linn. Soc.* **66,** 259–275 (1973).
10. Voznesenskaya, E. V., Franceschi, V. R., Pyankov, V. I. & Edwards, G. E. Anatomy, chloroplast structure and compartmentation of enzymes relative to photosynthetic mechanisms in leaves and cotyledons of species in the tribe Salsoleae (Chenopodiaceae). *J. Exp. Bot.* **50,** 1779–1795 (1999).
11. Voznesenskaya, E. V. & Gamaley, Y. V. The ultrastructural characteristics of leaf types with Kranz-anatomy. *Bot. Zh.* **71,** 1291–1307 (1986) (in Russian).
12. Pyankov, V. I. *et al.* Occurrence of C_3 and C_4 photosynthesis in cotyledons and leaves of *Salsola* species (Chenopodiaceae). *Photosynth. Res.* **63,** 69–84 (2000).
13. Kanai, R. & Edwards, G. in *C_4 Plant Biology* (eds Sage, R. F. & Monson, R. K.) 49–87 (Physiological Ecology series, Academic, San Diego, 1999).
14. Pyankov, V. I. *et al.* Features of photosynthesis in *Haloxylon* species of Chenopodiaceae that are dominant plants in Central Asian deserts. *Plant Cell Physiol.* **40,** 125–134 (1999).
15. Farquhar, G. D. On the nature of carbon isotope discrimination in C_4 species. *Aust. J. Plant Physiol.* **10,** 205–226 (1983).
16. Laing, W. A., Ogren, W. L. & Hageman, R. H. Regulation of soybean net photosynthetic CO_2 fixation by the interaction of CO_2, O_2, and ribulose 1,5-diphosphate carboxylase. *Plant Physiol.* **54,** 678–685 (1974).
17. Maroco, J. P., Ku, M. S. B. & Edwards, G. E. Utilization of O_2 in the metabolic optimization of C_4 photosynthesis. *Plant Cell Environ.* **23,** 115–121 (2000).
18. Cerling, T. E., Quade, J. & Wang, Y. Expansion and emergence of C_4 plants. *Nature* **371,** 112 (1994).
19. Pagani, M., Freeman, K. H. & Arthur, M. A. Late Miocene atmospheric CO_2 concentrations and the expansion of C_4 grasses. *Science* **285,** 876–878 (1999).
20. Sheehy, J. E., Mitchell, P. L. & Hardy, B. *Redesigning Rice Photosynthesis to Increase Yield* (IRRI and Elsevier Science, Makati City, Philippines, 2000).
21. Matsuoka, M., Furbank, R. T., Fukayama, H. & Miyao, M. Molecular engineering of C_4 photosynthesis. *Annu. Rev. Plant Physiol. Plant Mol. Biol.* **52,** 297–314 (2001).
22. Maurino, V. G., Drincovich, M. F. & Andreo, C. S. NADP-malic enzyme isoforms in maize leaves. *Biochem. Mol. Biol. Int.* **38,** 239–250 (1996).
23. Long, J. J., Wang, J.-L. & Berry, J. O. Cloning and analysis of the C_4 photosynthetic NAD-dependent malic enzyme of amaranth mitochondria. *J. Biol. Chem.* **269,** 2827–2833 (1994).
24. Voznesenskaya, E. V. *et al. Salsola arbusculiformis*, a C_3–C_4 intermediate in Salsoleae (Chenopodiaceae). *Ann. Bot.* **88,** 337–348 (2001).
25. Akhani, H., Trimborn, P. & Ziegler, H. Photosynthetic pathways in *Chenopodiaceae* from Africa, Asia and Europe with their ecological, phytogeographical and taxonomical importance. *Plant Syst. Evol.* **206,** 187–221 (1997).
26. Dai, Z., Ku, M. S. B. & Edwards, G. E. Oxygen sensitivity of photosynthesis in C_3, C_4, and C_3–C_4 intermediate species of *Flaveria*. *Planta* **198,** 563–571 (1996).

Acknowledgements

We thank the Electron Microscope Center of Washington State University for use of facilities and staff assistance. We thank N. Ogar and H. Akhani for supply of viable seeds, and S. Huber, C. A. Ryan and T. Okita for comments on the manuscript. This work was supported by the National Science Foundation (G.E.E.) and the DFG (H.F.).

Correspondence and requests for materials should be addressed to G.E. (e-mail: edwardsg@wsu.edu).

Interactive memory systems in the human brain

R. A. Poldrack*†, J. Clark*, E. J. Paré-Blagoev*†, D. Shohamy‡, J. Creso Moyano‡, C. Myers§ & M. A. Gluck‡

** Athinoula A. Martinos Center for Biomedical Imaging, Massachusetts General Hospital, and Harvard Medical School, Charlestown, Massachusetts 02131, USA*
† Harvard Graduate School of Education, Cambridge, Massachusetts 02138, USA
‡ Center for Molecular and Behavioural Neuroscience; and § Department of Psychology, Rutgers University, Newark, New Jersey 07102, USA

Learning and memory in humans rely upon several memory systems, which appear to have dissociable brain substrates[1,2]. A fundamental question concerns whether, and how, these memory systems interact. Here we show using functional magnetic resonance imaging (FMRI) that these memory systems may compete with each other during classification learning in humans. The medial temporal lobe and basal ganglia were differently engaged across subjects during classification learning depending upon whether the task emphasized declarative or nondeclarative memory, even when the to-be-learned material and the level of performance did not differ. Consistent with competition between

memory systems suggested by animal studies[3,4] and neuroimaging[5], activity in these regions was negatively correlated across individuals. Further examination of classification learning using event-related FMRI showed rapid modulation of activity in these regions at the beginning of learning, suggesting that subjects relied upon the medial temporal lobe early in learning. However, this dependence rapidly declined with training, as predicted by previous computational models of associative learning[6–8].

In experiment 1, we used FMRI to image brain activity during performance of classification tasks designed to emphasize either declarative or nondeclarative memory processes. Subjects engaged in a category learning ('weather prediction') task with probabilistic cue–outcome relations based on trial-by-trial feedback[9,10]. This type of task, which involves online learning of stimulus–response associations, is thought to engage nondeclarative memory[11,12], and previous research with this task revealed that patients with basal ganglia disorders were impaired[13,14]. Amnesic patients with damage to the medial temporal lobe (MTL) demonstrated normal learning during the early portion of training but were impaired relative to controls as learning progressed[10,13]. We compared performance of normal subjects on this feedback-based (FB) version of the weather-prediction task with performance on a version of the task designed to emphasize declarative memory processes (see Fig. 1). Rather than FB learning, subjects learned the stimuli and categories in a paired-associate (PA) manner and were then tested on their classification ability after learning. Paired-associate learning, which requires learning associations between previously unrelated pairings of stimuli, is thought to engage declarative memory, and is known to rely strongly upon the MTL[15,16]. Classification ability at the end of training was similar for both the FB and PA version of the task (86.5% for FB versus 82.7% for PA; $F_{1,21} = 1.13$, $P = 0.30$), suggesting that subjects in both tasks acquired knowledge capable of supporting comparable accuracy.

During FMRI scanning at 1.5 T in experiment 1, subjects alternated between the classification task and a baseline task with similar perceptual and motor characteristics but no learning demands. The FB and PA versions of the task (given to separate groups of 13 subjects) differed in the timing of category presentation and the nature of the response (see Fig. 1), but the stimuli used across the two versions of the task were identical and both required a button-press response. Statistical parametric mapping was performed to identify regions whose activity was significantly different between classification and baseline tasks (see Fig. 2). Engagement in the FB weather-prediction task resulted in activation of the basal ganglia (caudate nucleus) in addition to widespread activation of cortical regions compared to the baseline task. Conversely, activity during the FB task was significantly below baseline in a number of regions; many of these regions (medial frontal and parietal cortex, auditory cortex) are often deactivated during performance of demanding visual tasks, but in this case the MTL was also deactivated. This pattern of activity is consistent with a previous study of the FB task using a different baseline task[5].

In order to determine whether MTL deactivation was specific to FB learning, we compared activity during the FB task with that observed during the PA weather-prediction task in a separate group of subjects. Comparison between groups demonstrated significant task-dependent modulation of both the MTL (PA > FB) and the caudate nucleus (PA < FB) (see Fig. 2c). This difference in MTL and caudate responses between FB and PA tasks suggests that the effects of these structures are negatively related. Random-effects functional connectivity analysis was performed to determine more directly whether these regions exhibit negatively correlated activity. We extracted signal change for each subject from the left MTL region showing maximal task-dependent modulation in the PA > FB comparison (stereotactic coordinates [−33, −30, −18], 6 mm radius). We then entered the signal change data into a correlation analysis across subjects with signal change in all voxels. This analysis identified a right caudate region whose activity was negatively correlated with the left MTL, along with several other regions (see Fig. 2). Although this correlation cannot establish causation, it provides further evidence for a negative relationship between these structures.

These results suggest that engagement of the declarative and nondeclarative memory systems may be modulated by task demands when the material to be learned is identical. To determine whether the engagement of these systems changes dynamically over the course of learning, another group of 14 subjects participated in experiment 2 using event-related FMRI at 3 T with the FB task. The use of event-related FMRI allowed the decomposition of responses to individual trials, and further allowed parametric analysis of changes in the event-related response over the course of learning[17].

Subjects performed 96 classification trials over the course of two FMRI scans. As in experiment 1, the basal ganglia and other cortical and subcortical regions were active compared to baseline, and the MTL was deactivated (see Fig. 3). Examination of parametric changes (specifically, exponential changes) in the evoked response over time demonstrated that MTL was initially active and caudate was initially inactive, but that the MTL quickly became deactivated and the caudate nucleus became activated. We saw no parametric change in the MTL during the second block of trials (that is, the MTL was deactivated throughout), whereas the caudate nucleus did show a renewed dip and subsequent rise in the second block.

On the basis of the results from experiment 2, we re-analysed the data from the FB task in experiment 1 for parametric changes in response, using the regions identified in experiment 2 as a priori regions of interest (8-mm-diameter sphere centred at local maximum). A significant parametric increase was observed in the caudate nucleus region, confirming the rapid changes in caudate activity observed in the event-related study, whereas the parametric decrease in MTL was not significant ($P = 0.114$).

The results presented here provide the first substantive evidence, to our knowledge, for competition between memory systems in the

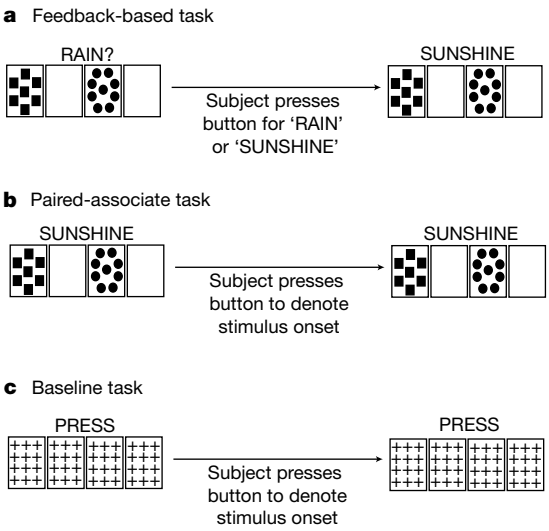

Figure 1 Depiction of task design for experiment 1. **a**, In the feedback-based (FB) task (also used in experiment 2), the stimulus was initially presented with a cue to respond (in this case, 'RAIN'), and the subject responded according to whether he/she thought the particular set of cards was associated with rain or sunshine by pressing one of two keys. The feedback (that is, the outcome for that trial) was then presented after 4 s. **b**, In the paired-associate (PA) task, the outcome was presented initially at the same time as the stimulus, and remained on the screen throughout the trial. Subjects pressed a single key simply to note the appearance of the stimulus. **c**, In the baseline task, subjects were presented with a set of crosshair stimuli (different from those used in the classification trials) and pressed a single key simply to note the appearance of the stimulus.

human brain. Whereas our previous work demonstrated MTL deactivation and striatal activation during classification learning[5], the present study provides direct evidence for competition at the neural level by demonstrating three essential features of the MTL–striatum interaction. First, it shows that engagement of MTL and striatum is modulated by whether the task encourages the use of declarative versus nondeclarative memory processes or strategies. Second, it demonstrates that engagement of these regions is negatively correlated across subjects. Third, it demonstrates rapid reciprocal changes in the engagement of these regions. These data are concordant with animal lesion studies demonstrating that the memory systems based on the MTL and striatum can compete with one another during learning[3,4,18].

Previous studies of classification learning found that patients with MTL lesions were impaired after several hundred training trials compared to matched controls[10,13]. These patients did not exhibit significant deficits in early training (through 50 trials), although subsequent studies have found early-learning deficits as well[19]. Patients with basal ganglia disorders (Parkinson's and Huntington's diseases) were severely impaired on the task from the onset of training and did not learn the task even after many training trials[13,14]. These findings have been taken to suggest that category learning relies primarily upon the striatum but that the MTL becomes important later in training[10,13]. The results of the present study, however, show that the MTL is engaged very early in learning and that it then becomes deactivated throughout training (up to 144 trials in experiment 1). Because the task used in the FMRI studies reported here differs in several ways from the version used in the

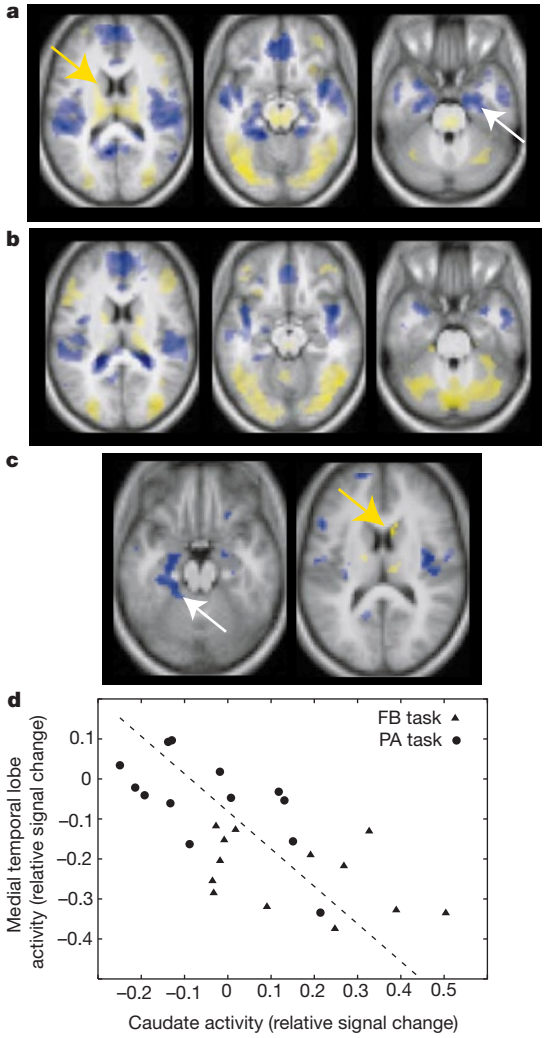

Figure 2 Results from FB versus PA classification learning (experiment 1). **a**, Activation for FB compared to baseline; areas in yellow were more active during weather prediction compared to baseline, whereas regions in blue were less active during weather prediction than baseline ($P < 0.005$ uncorrected, 5 voxel extent threshold). Yellow arrow highlights region of caudate activation, white arrow highlights region of MTL deactivation. **b**, Activation for PA compared to baseline. **c**, Regions exhibiting significant differences between FB and PA classification learning tasks. (yellow: FB > PA, blue: PA > FB). Yellow arrow highlights caudate region with FB > PA, white arrow highlights MTL region with PA > FB. **d**, Plot of task-related signal change from the MTL region exhibiting maximal task-dependent differences (centred at [–33, –30, –18], with a 6 mm radius) against a region in the right caudate that exhibited significant negative correlation with the MTL in functional connectivity analysis (centred at [9, 6, 21], with a 6 mm radius). Each data point represents a single subject.

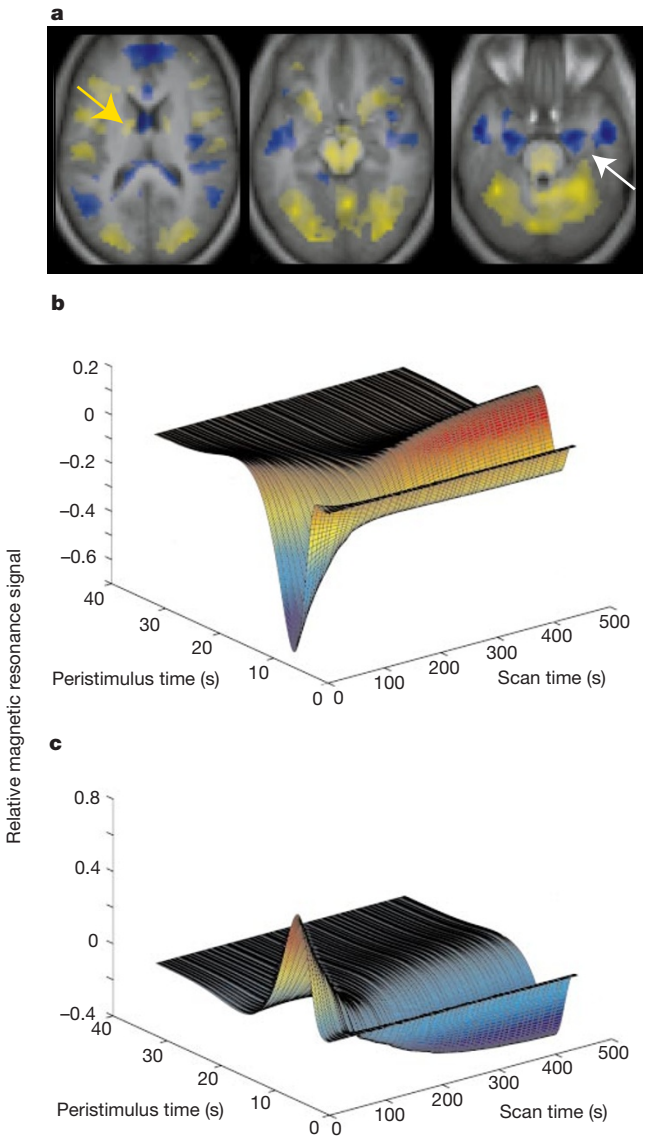

Figure 3 Results from event-related FMRI study of FB category learning (experiment 2). **a**, Regions exhibiting significant evoked activation (yellow) or deactivation (blue) for classification trials. Yellow arrow highlights region of caudate activation, white arrow highlights region of MTL deactivation. **b**, **c**, Depiction of parametric change in modelled evoked haemodynamic response across the initial 450-s scanning run (averaged across subjects) in **b**, left body of caudate nucleus (–12, 3, 21), and **c**, left MTL (–24, –3, –24). Red indicates positive, event-related response, blue indicates negative event-related response.

neuropsychological studies described above, the engagement of MTL and striatum may differ owing to procedural details. However, it is tempting to speculate that the late-learning deficit observed in patients with MTL lesions may be due to the absence of processes occurring early in training in normal individuals: that is, the MTL may not be strictly necessary for early learning, but its contributions during early learning may facilitate later learning. Evidence that MTL lesions may change the nature of early learning on classification tasks comes from Reber *et al.*[20], who found that MTL-lesioned patients showed normal early learning on the weather-prediction task but were impaired on transfer tests that required flexible use of knowledge acquired during learning.

The importance of MTL in early learning on the weather-prediction task was predicted by computational modelling of cortico-hippocampal interaction during learning[6–8]. These simulation studies predict that the classification task used here may require a significant degree of MTL mediation, owing to the many cue–cue configural regularities present in the stimulus set, but that the MTL is active only during early phases of learning in which new representations of the stimuli are being developed. Once new stimulus representations have been established early in learning, the model predicts that MTL involvement will decrease. These predictions are confirmed by the present FMRI results demonstrating that the MTL is initially active (during putative development of new stimulus representations) but subsequently decreases (after such representations stabilize). Analogous electrophysiological results have been found in rabbit eyeblink conditioning in which the hippocampal activity related to conditioned responses appears early in learning but disappears with extended training[21]. This computational theory interprets both the earlier animal data and the present human imaging data as implying an interaction between the hippocampus and other brain structures, in which the hippocampus has a modulatory role in learning by developing new stimulus representations during early phases of training which are used by the striatum to develop complex stimulus–response associations.

Competition between memory systems may reflect an adaptive mechanism for optimizing behaviour depending upon learning demands. Some animal studies[3,22,23] have shown that the MTL and striatum acquire different types of information during learning: the MTL appears to acquire flexible, relational knowledge (such as spatial relationships) whereas the striatum acquires inflexible stimulus–response associations. These differences have been most directly examined using a cross-maze learning task in rats. The rat is first taught to run to a particular arm of the maze from a given starting point, and is then tested by starting from a different location. The MTL supports place learning (in which the rat runs towards the previously rewarded spatial location from the new starting position) whereas the striatum supports response learning (in which the rat makes the previously rewarded motor response from the new starting position). Normal rats exhibit a transition from early reliance upon MTL-based place learning strategies to later reliance upon striatal-based response learning strategies[22,23]. Pharmacologic facilitation of MTL or suppression of striatum increases the later engagement of place strategies, whereas facilitation of striatum or suppression of MTL increases the early engagement of response strategies[22,23], suggesting that these structures are locked in a 'zero-sum' competition to control behaviour.

The interpretation of apparent task-related deactivations is complicated by the fact that such deactivations can reflect either active decreases during the task of interest or increases during the baseline task. In the present case there are two findings that suggest that the deactivations do not reflect increases during the baseline activity. First, MTL deactivation during the classification task has been found using three very different baseline tasks: counting the number of cards presented[5], simple button press (experiment 1), and visual fixation (experiment 2). Second, activation was modulated depending on task demands in experiment 1 (FB versus PA tasks) when the baseline task remained constant across these two tasks. Thus, we believe that the results reflect a specific decrease in FMRI signal during the classification task. However, the neurophysiological basis of this decrease remains unknown. In particular, there is current debate as to whether both excitatory and inhibitory synaptic activity result in increased FMRI signal[24,25]. Neural modelling suggests that the relation between FMRI signal and inhibition may depend upon features of local neural circuitry, such as the degree of recurrence[26]. Our results clearly demonstrate that MTL deactivation during FB learning reflects a response to task demands, but further work is necessary to understand fully the synaptic correlates of these signals.

Thus we have shown that learning involves competition between the MTL-based and striatal-based memory systems in the human brain. These findings provide a direct link to convergent findings of competitive memory systems in animal learning, and suggest that competition may serve as a mechanism to arbitrate between two fundamentally incompatible requirements of learning: the need for flexibly accessible knowledge (supported by the MTL) and the need to learn fast, automatic responses in specific situations (supported by the striatum). □

Methods

Subjects

A total of 40 right-handed subjects participated in the studies described here: 26 in experiment 1 (6 males, age range: 18–31) and 14 in experiment 2 (2 males, age range 19–33). All gave informed consent according to procedures approved by Massachusetts General Hospital.

Task and stimuli

In experiment 1, subjects participated in four scans lasting 468 s, during which they alternated every 26 s between the classification and baseline tasks. Subjects in the feedback-based group were asked to perform the classification task on each trial by pressing one of two buttons, and received feedback (category label) on each trial after 4 s. Those in the paired-associate group simply pressed a button to denote stimulus onset, and received the category label at trial onset (see Fig. 1). During the baseline task in both conditions, subjects were presented with a set of stimuli along with the instruction 'PRESS' and were asked simply to press a button to denote that the stimulus had appeared. For subjects in the PA group, learning was tested immediately after completion of the last scan by presenting all of the card combinations twice and asking subjects to classify each; no feedback was given.

In experiment 2, individual trials were presented as in experiment 1 (FB condition) but the interstimulus interval was varied across trials; the sequence of interstimulus intervals was determined by optimizing the design matrix for estimation of the FMRI response[27]. Event-related response was estimated in comparison to a baseline of visual fixation. Two scans lasting 450 s were performed with this task, with 48 trials occurring during each scan. Behavioural data were collected using a button box in the scanner; data for 3 subjects in experiment 1 (2 in the FB group and 1 in the PA group) were lost owing to computer malfunction.

Stimuli in both experiments were a set of four cards with geometric shapes (after ref. 10), any combination of which could appear on a given trial (except for all cards or none). Category labels were probabilistically associated with stimuli, with cue strengths of the individual cards specified as 80%, 60%, 40% and 20% respectively. These probabilities are slightly more extreme than those used in previous studies of this task[5,10], in order to encourage more consistent learning. Accuracy was determined according to a probability-maximizing metric, that is, responses that matched the most correct response for a given set of cards were counted as correct.

MRI acquisition

Twenty-one axial slices (5 mm thick, 1 mm gap) were collected at 1.5 T (Siemens Sonata; experiment 1) or 3 T (Siemens Allegra; experiment 2) using a gradient-echo echo-planar pulse sequence (repetition time, 2,000 ms; echo time, 40 ms (at 1.5 T) and 30 ms (at 3 T), field of view, 200 mm; matrix size, 64 × 64). High-resolution T1-weighted scans (MP-RAGE; Siemens) were acquired for anatomical localization.

Data analysis

Preprocessing and statistical analysis of the data were performed using SPM99 software (Wellcome Dept of Cognitive Neurology). Preprocessing included slice timing correction (experiment 2 only), motion correction, normalization to the MN1305 stereotactic space (interpolating to 3 mm cubic voxels) and spatial smoothing with an 8-mm gaussian kernel. Statistical analysis was performed using the general linear model. Global signal scaling was not applied, in order to prevent spurious deactivations. The design in experiment 1 was modelled using a boxcar function convolved with a canonical

haemodynamic response function, whereas the event-related design in experiment 2 was modelled using a canonical haemodynamic response and its temporal derivative[28]. Comparisons of interest were implemented as linear contrasts. This analysis was performed individually for each subject, and contrast images for each subject were used in a second-level analysis treating subjects as a random effect. Statistical maps were thresholded at $P < 0.005$ uncorrected for multiple comparisons with an extent threshold of 5 voxels. Tests on hypothesized regions were corrected for multiple comparisons ($P < 0.05$) using the gaussian-field small-volume correction in SPM99 after thresholding the statistical map at $P < 0.025$ with an extent threshold of 5 voxels. Parametric analysis was performed by including an additional regressor that modelled an exponentially changing HRF with a time constant of 100 s (ref. 17).

For functional connectivity analysis, signal from a seed region in the MTL (centred at −33, −30, −18, with a 6-voxel radius) was compared with all other voxels across subjects using simple correlation analysis, with a statistical parametric map determined for regions of significant positive or negative correlation[29].

Received 2 July; accepted 24 October 2001.

1. Gabrieli, J. D. Cognitive neuroscience of human memory. *Annu. Rev. Psychol.* **49,** 87–115 (1998).
2. Eichenbaum, H E. & Cohen, N. J. *From Conditioning to Conscious Recollection: Memory Systems of the Brain* (Oxford Univ. Press, New York, 2001).
3. Eichenbaum, H., Fagan, A., Mathews, P. & Cohen, N. J. Hippocampal system dysfunction and odor discrimination learning in rats: Impairment or facilitation depending on representational demands. *Behav. Neurosci.* **102,** 331–339 (1988).
4. Packard, M. G., Hirsh, R. & White, N. M. Differential effects of fornix and caudate nucleus lesions on two radial maze tasks: evidence for multiple memory systems. *J. Neurosci.* **9,** 1465–1472 (1989).
5. Poldrack, R. A., Prabakharan, V., Seger, C. & Gabrieli, J. D. E. Striatal activation during cognitive skill learning. *Neuropsychology* **13,** 564–574 (1999).
6. Gluck, M. & Myers, C. Hippocampal mediation of stimulus representation: A computational theory. *Hippocampus* **3,** 491–516 (1993).
7. Gluck, M. A., Oliver, L. M. & Myers, C. E. Late-training amnesic deficits in probabilistic category learning: a neurocomputational analysis. *Learn. Mem.* **3,** 326–340 (1996).
8. Gluck, M. A. & Myers, C. E. *Gateway to Memory: An Introduction to Neural Network Modeling of the Hippocampus and Learning* (MIT Press, Cambridge, Massachusetts, 2001).
9. Gluck, M. A. & Bower, G. H. From conditioning to category learning: an adaptive network model. *J. Exp. Psychol. Gen.* **117,** 227–247 (1988).
10. Knowlton, B., Squire, L. R. & Gluck, M. A. Probabilisitic classification in amnesia. *Learn. Mem.* **1,** 106–120 (1994).
11. Mishkin, M., Malamut, B. & Bachevalier, J. in *Neuropsychology of Memory* (eds Squire, L. R. & Butters, N.) 287–296 (Guilford, New York, 1984).
12. Squire, L. R. Memory and the hippocampus: A synthesis from findings with rats, monkeys, and humans. *Psychol. Rev.* **99,** 195–231 (1992).
13. Knowlton, B. J., Mangels, J. A. & Squire, L. R. A neostriatal habit learning system in humans. *Science* **273,** 1399–1402 (1996).
14. Knowlton, B. J. *et al*. Dissociations within nondeclarative memory in Huntington's disease. *Neuropsychology* **10,** 538–548 (1996).
15. Winocur, G. & Weiskrantz, L. An investigation of paired-associate learning in amnesic patients. *Neuropsychologia* **14,** 97–110 (1976).
16. Warrington, E. K. & Weiskrantz, L. Amnesia: A disconnection syndrome? *Neuropsychologia* **20,** 233–248 (1982).
17. Buchel, C., Holmes, A. P., Rees, G. & Friston, K. J. Characterizing stimulus-response functions using nonlinear regressors in parametric fMRI experiments. *Neuroimage* **8,** 140–148 (1998).
18. Kim, J. J. & Baxter, M. G. Multiple brain-memory systems: the whole does not equal the sum of its parts. *Trends Neurosci.* **24,** 324–330 (2001).
19. Hopkins, R., Myers, C., Shohamy, D. & Gluck, M. Impaired category learning in hypoxic subjects with hippocampal damage. *Soc. Neurosci. Abstr.* **27,** 347.5 (2001).
20. Reber, P. J., Knowlton, B. J. & Squire, L. R. Dissociable properties of memory systems: differences in the flexibility of declarative and nondeclarative knowledge. *Behav. Neurosci.* **110,** 861–871 (1996).
21. Sears, L. L. & Steinmetz, J. E. Acquisition of classically conditioned-related activity in the hippocampus is affected by lesions of the cerebellar interpositus nucleus. *Behav. Neurosci.* **104,** 681–692 (1990).
22. Packard, M. G. & McGaugh, J. L. Inactivation of hippocampus or caudate nucleus with lidocaine differentially affects expression of place and response learning. *Neurobiol. Learn. Mem.* **65,** 65–72 (1996).
23. Packard, M. G. Glutamate infused posttraining into the hippocampus or caudate-putamen differentially strengthens place and response learning. *Proc. Natl Acad. Sci. USA* **96,** 12881–12886 (1999).
24. Waldvogel, D. *et al*. The relative metabolic demand of inhibition and excitation. *Nature* **406,** 995–998 (2000).
25. Magistretti, P. J. & Pellerin, L. Cellular mechanisms of brain energy metabolism and their relevance to functional brain imaging. *Phil. Trans. R. Soc. Lond. B* **354,** 1155–1163 (1999).
26. Tagamets, M. & Horwitz, B. Interpreting PET and fMRI measures of functional neural activity: the effects of synaptic inhibition on cortical activation in human imaging studies. *Brain Res. Bull.* **54,** 267–273 (2001).
27. Dale, A. M. Optimal experimental design for event-related fMRI. *Hum. Brain Map.* **8,** 109–114 (1999).
28. Friston, K. J., Zarahn, E., Josephs, O., Hensen, R. N. & Dale, A. M. Stochastic designs in event-related fMRI. *Neuroimage* **10,** 607–619 (1999).
29. Horwitz, B., Mcintosh, A. R., Haxby, J. V. & Grady, C. L. Network analysis of brain cognitive function using metabolic and blood flow data. *Behav. Brain Res.* **66,** 187–193 (1995).

Acknowledgements

We thank N. J. Cohen, R. Raizada and A. Wagner for helpful comments. This work was supported by the Alafi Family Foundation and the Athinoula A. Martinos Center for Biomedical Imaging.

Competing interests statement

The authors declare that they have no competing financial interests.

Correspondence and requests for materials should be addressed to R.P. (e-mail: poldrack@nmr.mgh.harvard.edu).

Inhibitory PAS domain protein is a negative regulator of hypoxia-inducible gene expression

Yuichi Makino*†, Renhai Cao‡, Kristian Svensson§‖, Göran Bertilsson§‖, Mikael Åsman¶, Hirotoshi Tanaka†, Yihai Cao‡, Anders Berkenstam§‖ & Lorenz Poellinger*

** Department of Cell and Molecular Biology, Medical Nobel Institute; ‡ Department of Microbiology and Tumor Biology; and ¶ Center for Genomics and Bioinformatics, Karolinska Institutet, S-171 77 Stockholm, Sweden*
† Division of Clinical Immunology, Advanced Clinical Research Center, Institute of Medical Science, The University of Tokyo, 4-6-1 Shirokanedai, Minato-ku, Tokyo 108-8639, Japan
§ Pharmacia Corporation, S-112 87 Stockholm, Sweden

Alteration of gene expression is a crucial component of adaptive responses to hypoxia. These responses are mediated by hypoxia-inducible transcription factors (HIFs)[1,2]. Here we describe an inhibitory PAS (Per/Arnt/Sim) domain protein, IPAS, which is a basic helix-loop-helix (bHLH)/PAS protein structurally related to HIFs. IPAS contains no endogenous transactivation function but demonstrates dominant negative regulation of HIF-mediated control of gene expression. Ectopic expression of IPAS in hepatoma cells selectively impairs induction of genes involved in adaptation to a hypoxic environment, notably the vascular endothelial growth factor (VEGF) gene, and results in retarded tumour growth and tumour vascular density *in vivo*. In mice, IPAS was predominantly expressed in Purkinje cells of the cerebellum and in corneal epithelium of the eye. Expression of IPAS in the cornea correlates with low levels of expression of the VEGF gene under hypoxic conditions. Application of an IPAS antisense oligonucleotide to the mouse cornea induced angiogenesis under normal oxygen conditions, and demonstrated hypoxia-dependent induction of VEGF gene expression in hypoxic corneal cells. These results indicate a previously unknown mechanism for negative regulation of angiogenesis and maintenance of an avascular phenotype.

When screening mouse expressed sequence tag (EST) databases using hidden Markov model profiles[3] for HIF homology search, we identified an EST clone encoding a putative new protein, designated IPAS, containing a bHLH PAS motif. DNA sequence analysis demonstrated that IPAS complementary DNA contains an open reading frame of 921 nucleotides, encoding a polypeptide of 307 amino acids (Fig. 1a). Alignment analysis of this amino-acid sequence with known bHLH/PAS factors showed high similarity to HIF-1α[4] and HLF (HIF-α-like factor, also known as endothelial PAS domain protein 1, EPAS-1)[5,6] in the amino-terminal bHLH domain (75% and 76% identity, respectively; Fig. 1b), and to a lesser extent within the PAS region (34% and 36% in the PAS A domain, and 40% and 36% in the PAS B domain, respectively; Fig. 1b).

‖ Present addresses: Karobia AB, S-141 57 Huddinge, Sweden (A.B.); Neuronova AB, S-114 33 Stockholm, Sweden (G.B.); and Leica Microsystems AB, S-191 27 Sollentuna, Sweden (K.S.)